Physica Medica 62 (2019) 47–52

Contents lists available at ScienceDirect

Physica Medica

journal homepage: www.elsevier.com/locate/ejmp

Original paper

Quality assurance measurements of geometric accuracy for magnetic resonance imaging-based radiotherapy treatment planning

Iiro Ranta[a,b,c,*], Reko Kemppainen[d], Jani Keyriläinen[a,b,c], Sami Suilamo[b,c], Samuli Heikkinen[b], Mika Kapanen[e,f], Jani Saunavaara[b]

[a] Department of Physics and Astronomy, University of Turku, Vesilinnantie 5, FI-20014 Turku, Finland
[b] Department of Medical Physics, Turku University Hospital, Hämeentie 11, P.O. Box 52, FI-20521 Turku, Finland
[c] Department of Oncology and Radiotherapy, Turku University Hospital, Hämeentie 11, P.O. Box 52, FI-20521 Turku, Finland
[d] Philips MR Therapy Oy, Äyritie 4, FI-01510 Vantaa, Finland
[e] Department of Medical Physics, Medical Imaging Center, Tampere University Hospital, P.O. Box 2000, FI-33521 Tampere, Finland
[f] Department of Oncology, Unit of Radiotherapy, Tampere University Hospital, P.O. Box 2000, FI-33521 Tampere, Finland

ARTICLE INFO

Keywords:
Geometric distortion
Magnetic resonance imaging
Radiotherapy
MRI-only radiotherapy planning

ABSTRACT

Background: Using magnetic resonance imaging (MRI) as the only imaging method for radiotherapy treatment planning (RTP) is becoming more common as MRI-only RTP solutions have evolved. The geometric accuracy of MR images is an essential factor of image quality when determining the suitability of MRI for RTP. The need is therefore clear for clinically feasible quality assurance (QA) methods for the geometric accuracy measurement.
Materials and methods: This work evaluates long-term stability of geometric accuracy and the validity of a 2D geometric accuracy QA method compared to a prototype 3D method and analysis software in routine QA. The long-term follow-up measurements were conducted on one of the 1.5 T scanners over a period of 19 months using both methods. Inter-scanner variability of geometric distortions was also evaluated in three 1.5 T and three 3 T MRI scanners from a single vendor by using the prototype 3D QA method.
Results: The geometric accuracy of the magnetic resonance for radiotherapy (MR-RT) platform remained stable within 2 mm at distances of < 250 mm from isocenter. All scanners achieved good geometric accuracy with mean geometric distortions of < 1 mm at < 150 mm and < 2 mm at < 250 mm from the isocenter. Both measurement methods provided relevant information about geometric distortions.
Conclusions: Geometric distortions are often considered a limitation of MRI-only RTP. Results indicate that geometric accuracy of modern scanners remain within acceptable limits by default even after many years of clinical use based on the 3D QA evaluation.

1. Introduction

The use of magnetic resonance imaging (MRI) is becoming increasingly common as the only imaging method for external radiotherapy treatment planning (RTP) [1]. Recent studies have concluded that for the pelvic region both target localization and dose calculation accuracy of MRI-only based radiotherapy simulation is sufficient when compared to conventional computed tomography (CT)-based RTP [2–6]. This diminishes the need for CT in the RTP workflow. The use of a single imaging modality eliminates the error in target delineation caused by CT to MRI co-registration [7]. This is also more resource- and cost-efficient than the traditional combination of CT and MRI [1]. Moreover, the exposure of healthy tissue to ionizing radiation is consequently reduced. However, the use of MRI-only -based RTP workflow imposes stricter requirements on geometric accuracy.

Both external and internal factors may lead to changes in the geometric performance of a scanner. External factors include any ferromagnetic objects near the MRI suite. Internal factors include the drift of the static magnetic field or malfunction in gradient performance. Therefore, it is valuable to know if the geometric accuracy of older, same generation scanners is comparable to the accuracy of more recently installed systems.

While the feasibility of MRI-only RTP has been demonstrated for prostate and brain regions in recent studies [3,6–8], the adequacy of routine quality assurance (QA) methods for geometric accuracy is a concern in the use of MR images in RTP. Reproducibility of geometric distortions have been studied on permanent magnet systems [9]. However, there is little information concerning changes in geometric

* Corresponding author at: Department of Physics and Astronomy, University of Turku, Vesilinnantie 5, FI-20014, Finland.
E-mail address: iivera@utu.fi (I. Ranta).

https://doi.org/10.1016/j.ejmp.2019.04.022
Received 15 February 2019; Received in revised form 29 March 2019; Accepted 24 April 2019
Available online 09 May 2019

distortion on modern superconducting systems over an extended period of time. In addition, studies that evaluate the variation of system-induced geometric distortion between individual MRI scanners used for MRI-only RTP is limited [10,11]. It is now possible to purchase MRI-only product sets for older scanners that were originally installed for use in diagnostic imaging cases.

Compromises in geometric accuracy could also restrict the successful application of MRI-only -based RTP to other anatomical sites of the human body. Because there is growing interest in moving towards MRI-only planning [12,13] the need for a universal and feasible geometric accuracy QA method is emphasized.

Several studies evaluating three-dimensional (3D) geometric distortions have been conducted using various scanning methods and a multitude of designated 3D phantoms [14–19]. The use of 3D phantoms may be impractical for periodic clinical QA tests because of e.g. large size and laborious positioning of the phantoms. This increases the time and resources needed for the QA workflow. Thus, it is important to compare more user-friendly and faster methods for routine geometric accuracy QA that are sensitive enough to detect clinically meaningful changes in performance.

Philips MRCAT (magnetic resonance for calculating attenuation) [20] was the first commercial solution for the synthetic CT (sCT) generation. The MRCAT algorithm generates sCT images from acquired T1-weighted mDixon MR images. Therefore, the geometric uncertainties of MR images are directly transferred to geometric uncertainties of the sCT images used for RTP.

The main objective of this study is to evaluate the long-term stability of geometric accuracy of a 1.5 T Philips Ingenia MR-RT platform (Koninklijke Philips N.V., Amsterdam, The Netherlands). The scanner has been used routinely for MRI-only RTP scans since January 2016. By February 2019, over 300 MRI-only RT plans for prostate cancer patients have been generated using MRCAT method and used in clinical RT treatment. The clinical feasibility of a routine, two-dimensional (2D) geometric accuracy QA method, recommended by the vendor, is compared to a similar prototype 3D QA method as a part of the QA program of the MR-RT platform.

Another objective is to evaluate and compare the magnitude of scanner-induced geometric distortion of three 1.5 T and three 3.0 T Philips Ingenia MRI scanners. This includes the 1.5 T MR-RT platform, and five other scanners that are currently in diagnostic use.

2. Materials and methods

2.1. Phantoms and MRI equipment

Two phantoms designated for the measurement of geometric accuracy were used. The Philips 2D geometric QA phantom is a part of the commercial MRCAT solution. It consists of a single acrylic plate with a well-defined array of marker capsules and a base for the phantom attachment. The effective measurement area of the phantom is 500 mm × 450 mm. The capsules contain an oily solution to produce a signal similar to fatty tissue. Milled laser ridges are located on the phantom surface in transversal, sagittal and coronal plane directions to speed up the alignment of the phantom.

A prototype Philips 3D geometric QA phantom was used for the 3D QA measurements. The design of the 3D phantom resembles that of the 2D phantom, but it consists of seven identical acrylic plates that have a larger array of capsules with a total number of 1932 measurement points. This enables measurement of geometric distortions closer to the edges of the magnet bore. The 3D phantom capsules cover a cylindrical volume of 500 mm in diameter and 330 mm in length. Spacing between the plates is 55 mm. In both phantoms, the capsules are spaced in a 25 mm × 25 mm array. The phantoms are presented in Fig. 1.

The 1.5 T MR-RT platform was used for the long-term geometric accuracy monitoring.

During the monitoring period of 19 months, 2D and 3D QA measurements were performed five times, roughly every three months to evaluate the stability of geometric accuracy of the system and the feasibility of the 2D QA method compared to the 3D QA method in clinical QA.

For scanner dependent geometric accuracy comparison, 3D QA measurements were performed once for three Philips Ingenia 1.5 T MRI and three Philips Ingenia 3.0 T MRI devices at Turku University Hospital (Turku, Finland) and at Philips MR Therapy Oy facility (Vantaa, Finland). The scanners were installed between the years 2011 and 2016.

2.2. Imaging

A flat patient couch top intended for use in RTP imaging was used for positioning the phantom in all QA sessions instead of a standard curved patient couch used in diagnostic imaging. Integrated dS T/R System Body coil was used for acquisition in both 1.5 T and 3 T systems. The manufacturer's 3D gradient nonlinearity correction algorithm was used in all measurements. Active shimming was not performed prior to any of the QA scans. The essential imaging parameters of 2D and 3D QA scan protocols are presented in Table 1.

During the 5th month (January 16th, 2017) of the 19-month monitoring period, the MR-RT platform suffered an unintentional quench of the static magnetic field due to human error during electricity work. This did not cause any external damage to the system and gave an additional opportunity to monitor the scanner performance before and after a major technical failure and its possible effects on the geometric accuracy.

2.2.1. 3D QA for geometric accuracy

The 3D QA scans were performed by positioning the central acrylic plate to the isocenter. During the QA scan, the acrylic plates were imaged using a single large-stack 3D GRE sequence. The phantom was stationary throughout the scanning procedure. Manual phantom positioning with scout images was used due to variable accuracy of the in-bore laser systems. This improved the positioning consistency between the diagnostic scanners.

The 3D QA scan images were analyzed using vendor's designated command prompt-based QA analysis and program. The analysis program identified the location of a single marker by calculating the pixel intensity-weighted centre of gravity over a predefined 3D ROI covering the marker and generated a marker coordinate file [21]. During distortion evaluation, marker coordinates determined from the 3D QA scan images were compared to reference marker positions included in the QA software. This produced the 3D distortion information. Global offsets resulting from positioning error compared to reference were also detected by the analysis software and subtracted from the final distortion results. It is possible that in the very peripheries of the magnet bore, where the most severe distortions are present, the detection algorithm may underestimate the true maximum distortion as some of the fiducial markers cannot be reliably detected. This can be either due to poor signal or aliasing of two or more fiducial markers. Total distortions at these locations can be estimated to be > 12 mm.

Determination of the average geometrical distortion at different distances from the isocenter was performed by defining four individual ranges of interest: 100–150 mm, 150–200 mm, 200–250 mm and 250–290 mm from the isocenter. The data points in the range of 0–100 mm from the isocenter were ignored, as the distortions in the center of FOV are the smallest.

Mean total distortion and standard deviation values for every range were calculated for each scanner. A scatter plot of the total geometric distortion as a function of the above described data points was also generated for all ranges of interest. When comparing the measured QA data to an ideal reference, the mechanical inaccuracies of the 3D phantom are reflected in the distortion results.

The 2D geometric accuracy QA method evaluates only in-plane

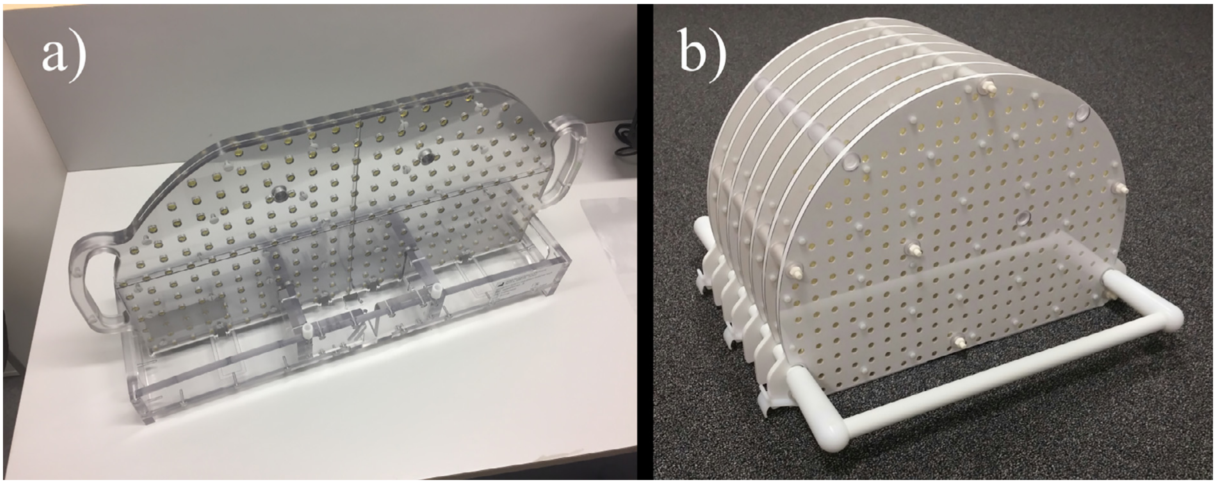

Fig. 1. a) The 2D geometric QA phantom. b) The 3D geometric QA phantom.

Table 1
The MRI sequences and parameters. Bracketed values were used with 3 T devices.

Sequence	Name®	TE (ms)	TR (ms)	Flip angle (°)	Acq. Matrix	Voxel size (mm)	Slice thickness, gap (mm)	Image stacks, slices	BW/px (Hz)
T_1-w 3D GRE	3D geometric fidelity QA	3.4	6.7	15	512	1.09 × 1.09 × 1.00	2, −1	1, 400	431 (862)
T_1-w 3D GRE	2D geometric fidelity QA	3.4	6.7	15	512	1.09 × 1.09 × 1.00	2, −1	7, 25	217

Table 2
The results for 3D QA method measurements. a) Mean 3D geometric distortions per distance range and QA session for the 1.5 T MR-RT platform. b) Mean 3D geometric distortions per distance range for the 1.5 T and 3 T scanners. c) Mean through-plane distortions per distance range for the 1.5 T and 3 T scanners. In all tables, μ represents the mean, σ is represents the standard deviation and 95% max. is the 95th percentile of the distortion per given distance interval.

a)

Scan date	Distance from isocenter [mm]											
	100–150			150–200			200–250			250–290		
	μ [mm]	σ [mm]	95% max. [mm]	μ [mm]	σ [mm]	95% max. [mm]	μ [mm]	σ [mm]	95% max. [mm]	μ [mm]	σ [mm]	95% max. [mm]
0 months	0.58	0.23	0.99	0.93	0.49	1.91	1.42	0.60	2.52	2.91	1.06	4.83
4 months	0.48	0.22	0.86	0.83	0.41	1.65	1.35	0.55	2.32	2.76	1.00	4.71
6 months	0.63	0.23	0.97	0.99	0.42	1.66	1.46	0.55	2.38	2.91	0.96	4.71
12 months	0.66	0.24	1.03	1.03	0.43	1.73	1.51	0.56	2.45	2.94	0.98	4.84
15 months	0.67	0.24	1.05	1.04	0.43	1.81	1.53	0.59	2.55	2.86	1.02	4.62

b)

Scanner	Distance from isocenter [mm]											
	100–150			150–200			200–250			250–290		
	μ [mm]	σ [mm]	95% max. [mm]	μ [mm]	σ [mm]	95% max. [mm]	μ [mm]	σ [mm]	95% max. [mm]	μ [mm]	σ [mm]	95% max. [mm]
3 T scanner #1	0.84	0.32	1.47	1.25	0.49	2.14	1.79	0.73	3.03	2.89	1.78	5.47
3 T scanner #2	0.74	0.26	1.20	1.11	0.37	1.73	1.62	0.49	2.44	3.56	3.13	7.66
3 T scanner #3	0.83	0.28	1.28	1.27	0.40	1.98	1.81	0.54	2.74	3.50	2.93	7.09
1.5 T scanner #1	0.67	0.26	1.16	1.05	0.38	1.76	1.57	0.55	2.43	2.76	1.11	5.07
1.5 T scanner #2	0.61	0.23	0.99	0.95	0.33	1.50	1.43	0.48	2.18	2.66	1.19	4.73
1.5 T MR-RT average	0.60	0.23	0.98	0.96	0.44	1.75	1.45	0.57	2.44	2.88	1.00	4.74

c)

Scanner	Distance from isocenter [mm]											
	100–150			150–200			200–250			250–290		
	μ [mm]	σ [mm]	95% max. [mm]	μ [mm]	σ [mm]	95% max. [mm]	μ [mm]	σ [mm]	95% max. [mm]	μ [mm]	σ [mm]	95% max. [mm]
3 T scanner #1	0.55	0.38	1.35	0.81	0.55	1.85	1.21	0.83	2.65	1.44	1.21	3.20
3 T scanner #2	0.33	0.23	0.76	0.47	0.33	1.08	0.88	0.50	1.66	1.85	3.01	6.00
3 T scanner #3	0.30	0.20	0.64	0.50	0.34	1.06	0.95	0.52	1.80	1.86	2.78	4.44
1.5 T scanner #1	0.47	0.32	1.04	0.67	0.45	1.48	1.02	0.62	2.05	1.24	0.77	2.51
1.5 T scanner #2	0.29	0.20	0.65	0.40	0.29	0.96	0.69	0.44	1.49	0.98	0.73	2.21
1.5 T MR-RT average	0.34	0.23	0.74	0.53	0.38	1.24	0.90	0.57	1.82	1.16	0.70	2.24

distortions (i.e. xy-plane) compared to real 3D measurement of the 3D QA method. Estimating the contribution of the through-plane distortion (i.e. parallel to z-axis) to the total geometric distortion is essential when factoring the interchangeability of the two methods. Therefore, through-plane distortions with respective averages and standard deviations were calculated separately.

2.2.2. 2D QA for geometric accuracy

The feasibility of the 2D geometric QA phantom as a part of the current MRCAT geometric QA method was evaluated by comparing it qualitatively to the 3D QA method. The areas of interest were the edge regions of the field-of-view (FOV) and the magnitude of distortion at greater radial distances from the magnet isocenter. The 2D geometric accuracy data were acquired by scanning the 2D phantom using specifically designed manufacturer's QA protocol for geometric accuracy. The QA measurements were conducted on a 1.5 T Philips Ingenia MR-RT platform with an external laser positioning system (ELPS) (LAP GmbH Laser Applikationen, Lueneburg, Germany) for RT positioning. The 2D QA scan protocol consisted of multiple identical T_1-weighted gradient-echo (GRE) sequences. During the automated QA scan, a series of images was acquired at seven different distances from the magnet's isocenter: z = 0 mm, ± 60 mm, ± 130 mm and ± 200 mm.

The analysis of the 2D QA images was performed automatically by the software during the QA protocol. The calculated magnitude of in-plane distortions can then be evaluated qualitatively by observing distortion isocontour lines of 1 mm, 2 mm, 3 mm and 5 mm in transverse images of the center slices at aforementioned distances from the isocenter. During the analysis, the volumetric 3D image stack is projected onto 2D plane along the z-axis. As a result, the through-plane distortion cannot be evaluated.

The reproducibility of the 2D QA measurement and assessment of error sources, i.e. noise and phantom positioning was tested in one of the QA sessions by repeating the 2D QA measurement three times without repositioning the phantom between the scans. After this the phantom was repositioned and the QA scan was repeated once more.

3. Results

3.1. 3D geometric QA

The results in Tables 2(a)–(b) and respective Fig. 2(a)–(b) show that the geometric performance of the 1.5 T MR-RT platform remained very stable throughout the 19-month monitoring period. When comparing geometric accuracy of the 1.5 T MR-RT platform to two diagnostic 1.5 T scanners, the results are almost identical. This was expected, as the only major technical difference between the scanners was the ELPS of the MR-RT platform.

Tested 1.5 T scanners generally performed better than 3 T scanners at distances ranging from 100 mm to 250 mm from the isocenter. At greater distances, the advantage begins to diminish as the data points near the edges of magnet bore demonstrate. As a result, the deviation of results with all the devices increases, because the valid data points are located across the FOV.

Scatter plot examples of 3D QA results are presented in supplementary Fig. 1. The results in Table 2(c) show the contribution of through-plane distortion to the total distortion.

3.2. 2D geometric QA

The MR-RT platform's 2D QA results reflect the results of the 3D QA measurements in Fig. 2(b), showing stable geometric performance throughout the monitoring period. Excerpts from the results are illustrated in Fig. 3 and in supplementary Figs. 2 and 3. The 2D QA images clearly show the decrease of the effective axial FOV as the distance from the isocenter grows, and the rapid increase in magnitude of geometric distortions. At transverse slice distances ranging from 0 to ± 130 mm, the distortions were limited to ≤ 3 mm in all measurements across the phantom.

4. Discussion

The 3D QA scans were performed successfully and distortions at different distances could be determined for all scanners. Examination of the results shows that even the older 1.5 T and 3 T scanners reached similar performance in comparison to newer scanners of the same hardware generation. This indicates that the geometric accuracy of the scanners remains stable after several years of regular use. Furthermore, it seems that the unintentional quench of the magnetic field did not cause changes to the geometric performance of the 1.5 T MR-RT platform.

Comparison between scanners shows that 1.5 T scanners are geometrically as accurate as 3 T scanners when the distance from the isocenter is less than 250 mm, as the differences are in the order of submillimeters. The increase in distortion magnitude as a function of distance from isocenter is also expected even when the manufacturer's gradient non-linearity correction algorithm is used.

In addition, some residual distortion remains from static field inhomogeneity, non-corrected gradient distortion and patient-induced

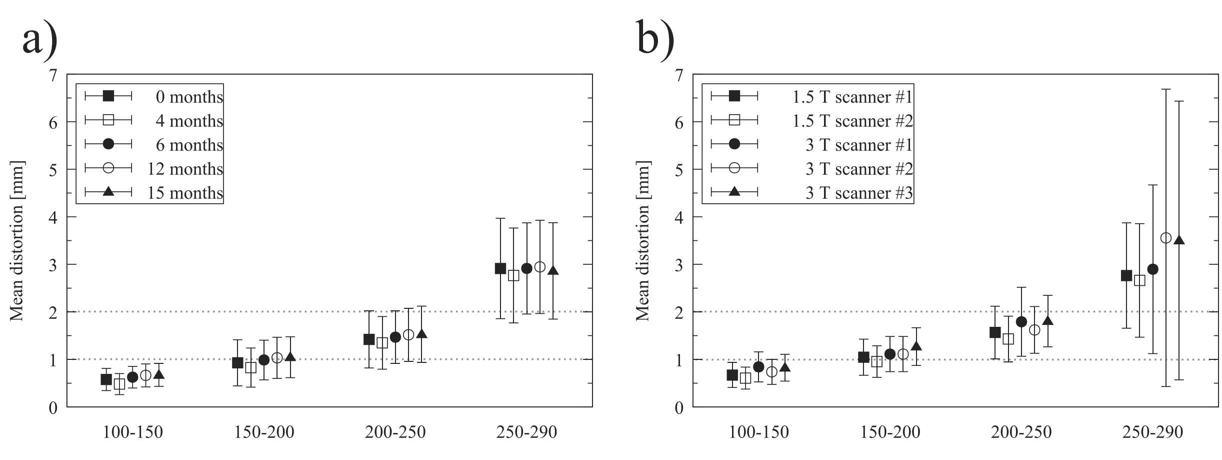

Fig. 2. a) Evolution of 1.5 T MR-RT platform's mean 3D geometric distortion including respective standard deviations. An unintended quenching of the magnetic field occurred during the 7th month of the long-term monitoring period. b) The 3D QA results for mean total distortion including respective standard deviations for five diagnostic MRI scanners.

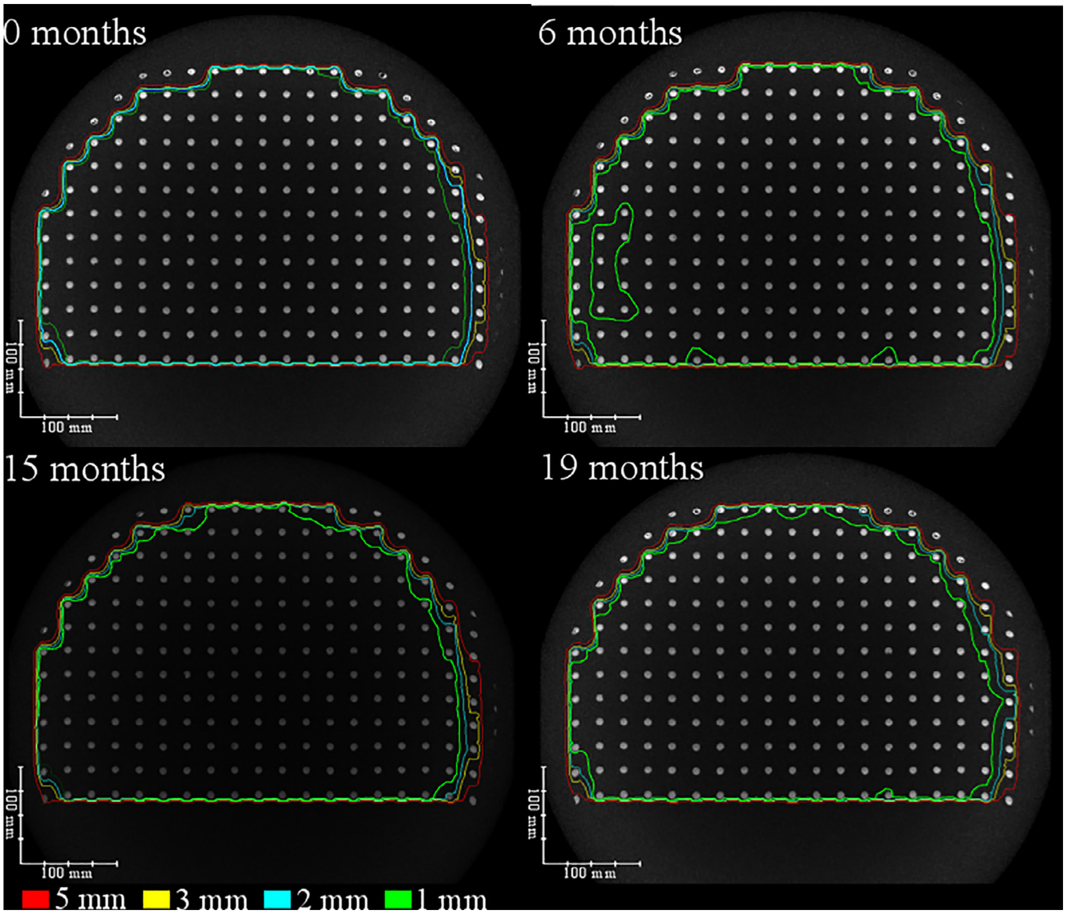

Fig. 3. Examples of analyzed images acquired with the 2D QA test protocol during the 19-month monitoring period. The lines illustrate the magnitude of maximum geometric distortion inside the defined area at a transverse distance of −130 mm from the magnet's isocenter.

distortion [11,22]. Patient-induced distortion is the most significant source of scanner-independent distortion that cannot be evaluated using phantoms. Our results also contain the mechanical inaccuracies of the 3D phantom, because calibration or a CT verification was not used for the 3D QA phantom.

The feasibility evaluation of the 2D QA method compared to the 3D method proved valuable in a clinical context. Based on our experience the 2D QA method is a repeatable and user-friendly way to measure distortions in routine clinical use due to a simpler design with only a single acrylic plate. Random error may be caused because of the possible misalignment of the base. However, geometric distortion measurements done using a large FOV 3D phantom have been demonstrated to be insensitive to small positioning uncertainties when the distortion measurement is based on deformable registration to a reference image [27]. In our study, these uncertainties are corrected by the analysis software when global offsets are subtracted.

A limitation of the 2D phantom-based QA method is that it does not evaluate through-plane (z-directional) distortion. Due to the nature of electromagnetic fields, however, the distortions in longitudinal direction would also manifest itself simultaneously with in-plane distortions. Thus, any 3D distortion is also detectable using 2D measurements. The detection sensitivity of distortions in 2D is inferior to the true quantitative 3D measurement, but for clinical QA purposes it is sufficient. The 2D QA method can therefore be used to verify geometric stability, once sufficient geometric accuracy has been demonstrated with a quantitative 3D QA measurement.

However, the 2D QA phantom setup is designed in such a way that repeatable orientation and scanning the phantom in sagittal and coronal directions is possible. The 2D QA protocol and analysis tool should therefore be developed so that automatic measurements in sagittal and coronal directions could be routinely performed. The 3D measurements are useful in more thorough QA sessions performed by physicists or technicians. Furthermore, the availability of lightweight, large FOV 3D distortion phantoms has been improving [28].

The results presented in this study are in line with the earlier research in which the scanner-induced geometric distortion of 1.5 T and 3 T devices were measured using various methods [10,16,18,22,23]. In the majority of these studies, imaging was performed using GRE-based sequences which further improves the comparability of our results to earlier research in the field. Differences between GRE and TSE-based sequences have also been shown to be small [10,17]. In general, the geometric accuracy of large FOV is important only for sequences that are used for the sCT generation. Our results are in good agreement with studies that investigate the feasibility of MRI-only RTP for brain and prostate regions [3,5–8]. Geometric accuracy is within 1 mm when volume of the head (radius < 150 mm) is considered and typically within 2 mm, when dimensions of the pelvic area (radius < 250 mm) are considered.

Establishing QA action limits for scanner-induced geometric distortion can be done based on the clinical RTP requirements, or previous research of the scanner-induced distortion effects in MRI-only RTP. Using stereotactic techniques commonly requires that the total spatial uncertainty from all sources should be < 1 mm. Therefore, geometric distortions ≤0.5 mm should be the minimum requirement for stereotactic RTP targets < 20 mm in diameter [11]. Based on our results these conditions can be met in the vicinity of the isocenter.

For pelvic region, geometric distortions of ≤2 mm at a radius < 250 mm could be considered adequate as a general guideline. This requirement can be justified by evaluating previous feasibility research of MRI-only dose calculation accuracy. A mean body outline error of ≤ 2 mm around the planning area resulted in mean dose differences of < 1% on the planning target volume (PTV) and organs-at-risk (OAR) areas compared to the CT-based RTP [5,24–26].

The results in this study demonstrate sufficient geometric accuracy for MRI-only RTP in all tested scanners and it seems that purchasing an RT option would a viable solution for older scanners due to the demonstrated stability of geometric accuracy. However, the geometric performance of every intended MR-RT platform should always be tested individually. Regular QA measurements of geometric accuracy are to be recommended, but our results indicate that stability is not an issue if the scanner performance is normal. Normal performance can be verified through regular American College of Radiology (ACR) phantom QA testing [29], for example.

In this study, it has been assumed that the same system induced distortions apply for the relevant MRI sequences used for RT. Effectively, this implies that the same receiver bandwidth must be used between the sequences. For sequence types that are more prone to distortions, additional assessments should be performed. It is also worth emphasizing that the analysis only measured the scanner-induced distortion including the mechanical inaccuracies of the phantom and evaluated the geometric performance of the tested MRI systems in general from QA perspective. Further studies are required to confirm the findings with systems from other manufacturers and to extend our results to those.

It can be concluded that based on the results of the investigated modern scanners, the long-term changes in magnetic field inhomogeneities and geometric accuracy of MR images are not severe. In addition, scanner-dependent variation of geometric accuracy was found to be minor, which could enable sites with existing current-generation scanners to acquire just RT options. Comparison between 2D phantom and 3D phantom-based QA results suggests that with improvements, the used 2D phantom QA method would be sufficient for clinical QA and stability monitoring in clinical MR-RT workflow.

Acknowledgements

The authors thank their co-workers at the University of Turku and Turku University Hospital (Turku, Finland). The authors also would like to thank Marko Pesola, Panu Vesanen and Lizette Warner of Philips MR Therapy Oy for their consultation, and Elizabeth Nyman of the Centre for Language and Communication Studies of University of Turku for performing the language check for the manuscript.

Disclosure of interest

R. Kemppainen is an employee of Philips MR Therapy Oy, Finland.

Appendix A. Supplementary data

Supplementary data to this article can be found online at https://doi.org/10.1016/j.ejmp.2019.04.022.

References

[1] Schmidt M, Payne G. Radiotherapy planning using MRI. Phys Med Biol 2015;60:R323. https://doi.org/10.1088/0031-9155/60/22/R323.

[2] Kapanen M, Tenhunen M. T1/T2*-weighted MRI provides clinically relevant pseudo-CT density data for the pelvic bones in MRI-only based radiotherapy treatment planning. Acta Oncol 2013;52(3):612–8. https://doi.org/10.3109/0284186X.2012.692883.

[3] Korhonen J, Kapanen M, Sonke J-J, Wee L, Salli E, Keyriläinen J, et al. Feasibility of MRI-based reference images for image-guided radiotherapy of the pelvis with either cone-beam computed tomography or planar localization images. Acta Oncol 2014;54(6):889–95. https://doi.org/10.3109/0284186X.2014.958197.

[4] Maspero M, van den Berg C, Landry G, Belka C, Parodi K, Seevinck P, et al. Feasibility of MRI-only proton dose calculations for prostate cancer radiotherapy using a commercial pseudo-CT generation method. Phys Med Biol 2017;62(24):9159–76. https://doi.org/10.1088/1361-6560/aa9677.

[5] Kemppainen R, Suilamo S, Tuokkola T, Lindholm P, Deppe MH, Keyriläinen J. Magnetic resonance-only simulation and dose calculation in external beam radiation therapy: a feasibility study for pelvic cancers. Acta Oncol 2017;56(6):792–8. https://doi.org/10.1080/0284186X.2017.1293290.

[6] Edmund JM, Nyholm T. A review of substitute CT generation for MRI-only radiation therapy. Radiat Oncol 2017;12:28. https://doi.org/10.1186/s13014-016-0747-y.

[7] Jonsson JH, Karlsson MG, Karlsson M, Nyholm T. Treatment planning using MRI data: an analysis of the dose calculation accuracy for different treatment regions. Radiat Oncol 2010;5(1):62. https://doi.org/10.1186/1748-717X-5-62.

[8] Koivula L, Wee L, Korhonen J. Feasibility of MRI-only treatment planning for proton therapy in brain and prostate cancers: dose calculation accuracy in substitute CT images. Med Phys 2016;43(8):4634–42. https://doi.org/10.1118/1.4958677.

[9] Mizowaki T, Nagata Y, Okajima K, Kokubo M, Negoro Y, Araki N, et al. Reproducibility of geometric distortion in magnetic resonance imaging based on phantom studies. Radiother Oncol 2000;57(2):237–42. https://doi.org/10.1016/S0167-8140(00)00234-6.

[10] Walker A, Liney G, Metcalfe P, Holloway L. MRI distortion: considerations for MRI based radiotherapy treatment planning. Australas Phys Eng Sci Med 2014;37:103–13. https://doi.org/10.1007/s13246-014-0252-2.

[11] Pappas E, Alshanqity, Moutsatsos A, Moutsatsos A, Lababidi H, Alsafi K, et al. MRI-related geometric distortions in stereotactic radiotherapy treatment planning: evaluation and dosimetric impact. Technol Cancer Res Treat 2017;16(6):1120–9. https://doi.org/10.1177/1533034617735454.

[12] Owrangi A, Greer P, Glide-Hurst C. MRI-only treatment planning: benefits and challenges. Phys Med Biol 2018;63. https://doi.org/10.1088/1361-6560/aaaca4. 05TR01.

[13] Weygand J, Fuller C, Ibbott G, Abdallah M, Ding Y, Jinzhong Y, et al. Spatial precision in magnetic resonance imaging-guided radiotherapy: the role of geometric distortions. Int J Rad Onc Biol Phys 2016;95(4):1304–16. https://doi.org/10.1016/j.ijrobp.2016.02.059.

[14] Stanescu T, Jans HS, Pervez N, Stavrev P, Fallone BG. A study on the magnetic resonance imaging (MRI)-based radiation treatment planning of intracranial lesions. Phys Med Biol 2008;53(13):3579–93. https://doi.org/10.1088/0031-9155/53/13/013.

[15] Breeuwer M, Holden M, Zylka W. Detection and correction of geometric distortion in 3D MR images. Proc. SPIE 4322, Medical Imaging 2001: Image Processing. 2001 Jul 3; San Diego, CA, USA;2001. https://doi.org/10.1117/12.430986.

[16] Wang D, Strugnell W, Cowin G, Doddrell DM, Slaughter R. Geometric distortion in clinical MRI systems: part I: evaluation using a 3D phantom. Magn Reson Imaging 2004;22(9):1211–21. https://doi.org/10.1016/j.mri.2004.08.012.

[17] Torfeh T, Hammoud R, Perkins G, McGarry M, Aouadi S, Celik A, et al. Characterization of 3D geometric distortion of magnetic resonance imaging scanners commissioned for radiation therapy planning. Magn Reson Imaging 2016;34(5):645–53. https://doi.org/10.1016/J.MRI.2016.01.001.

[18] Walker A, Liney G, Holloway L, Dowling J, Rivest-Henault D, Metcalfe P. Continuous table acquisition MRI for radiotherapy treatment planning: distortion assessment with a new extended 3D volumetric phantom. Med Phys 2015;42(4):1982–91. https://doi.org/10.1118/1.4915920.

[19] Huang K, Cao Y, Baharom U, Balter JM. Phantom-based characterization of distortion on a magnetic resonance imaging simulator for radiation oncology. Phys Med Biol 2016;61(2):774–90. https://doi.org/10.1088/0031-9155/61/2/774.

[20] Köhler M, Vaara T, van Grootel M, Hoogeveen R, Kemppainen R, Renisch S. MR-only simulation for radiotherapy planning [white paper]. Koninklijke Philips N.V., Vantaa, Finland. 2015 [cited 2019 Feb 12]. Available from: http://clinical.netforum.healthcare.philips.com/us_en/Explore/White-Papers/MRI/MR-only-simulation-for-radiotherapy-planning.

[21] Philips Medical Systems MR Finland. 3D Geometric QA for research use [user manual]. Vantaa, Finland: Koninklijke Philips N.V.; 2016.

[22] Stanescu T, Jans H-S, Wachowicz K, Fallone G. Investigation of a 3D system distortion correction method for MR images. J Appl Clin Med Phys 2010;11(1):200–16. https://doi.org/10.1120/jacmp.v11i1.2961.

[23] Sun J, Dowling J, Pichler P, Menk F, Rivest-Henault D, Lambert J, et al. MRI simulation: end-to-end testing for prostate radiation therapy using geometric pelvic MRI phantoms. Phys Med Biol 2015;60(8):3097–109. https://doi.org/10.1088/0031-9155/60/8/3097.

[24] Adjeiwaah M, Bylund M, Lundman JA, Thellenberg Karlsson C, Jonsson JH, Nyholm T. Quantifying the effect of 3T MRI residual system and patient-induced susceptibility distortions on radiotherapy treatment planning for prostate cancer. Int J Rad Onc Biol Phys 2017;100(2):317–24. https://doi.org/10.1016/j.ijrobp.2017.10.021.

[25] Gustafsson C, Nordström F, Persson E, Brynolfsson J, Olsson LE. Assessment of dosimetric impact of system specific geometric distortion in an MRI only based radiotherapy workflow for prostate. Phys Med Biol 2017;62(8):2976–89. https://doi.org/10.1088/1361-6560/aa5fa2.

[26] Kraus K, Jäkel O, Niebuhr N, Pfaffenberger A. Generation of synthetic CT data using patient specific daily MR image data and image registration. Phys Med Biol 2017;62(4):1358–77. https://doi.org/10.1088/1361-6560/aa5200.

[27] Wyatt J, Hedley S, Johnstone E, Speight R, Kelly C, Henry A, et al. Evaluating the repeatability and set-up sensitivity of a large field of view distortion phantom and software for magnetic resonance-only radiotherapy. Phys Imaging Radiat Oncol 2018;6:31–8. https://doi.org/10.1016/j.phro.2018.04.005.

[28] Spectronic Medical Ab, Sweden. GRADE phantoms and evaluation software, http://www.spectronic.se/wb/page-2/page10/index.html [accessed 15.3.2019].

[29] American College of Radiology. Phantom Test Guidance for Use of the Large MRI Phantom for the ACR MRI Accreditation Program, https://www.acraccreditation.org/-/media/ACRAccreditation/Documents/MRI/LargePhantomGuidance.pdf [accessed 15.3.2019].